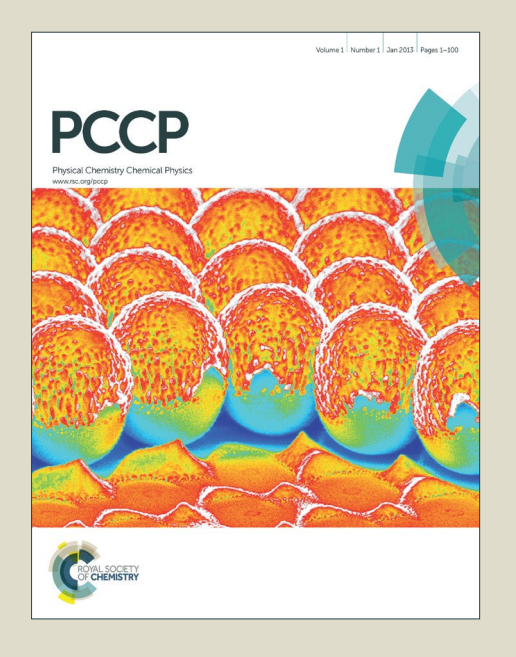


# Accepted Manuscript



This is an *Accepted Manuscript*, which has been through the Royal Society of Chemistry peer review process and has been accepted for publication.

Accepted Manuscripts are published online shortly after acceptance, before technical editing, formatting and proof reading. Using this free service, authors can make their results available to the community, in citable form, before we publish the edited article. We will replace this Accepted Manuscript with the edited and formatted Advance Article as soon as it is available.

You can find more information about *Accepted Manuscripts* in the **Information for Authors**.

Please note that technical editing may introduce minor changes to the text and/or graphics, which may alter content. The journal's standard <u>Terms & Conditions</u> and the <u>Ethical guidelines</u> still apply. In no event shall the Royal Society of Chemistry be held responsible for any errors or omissions in this *Accepted Manuscript* or any consequences arising from the use of any information it contains.



# A Theoretical Study of O<sub>2</sub> Activation by Au<sub>7</sub>-Cluster on Mg(OH)<sub>2</sub>: Roles of Surface Hydroxyls and Hydroxyl Defects

Chuanyi Jia a,b) \*, Weiliu Fan c) \*

- a) Guizhou Provincial Key Laboratory of Computational Nano-material Science, Institute of Applied Physics, Guizhou Normal College, Guiyang, 550018, China
- b) Guizhou Synergetic Innovation Center of Scientific Big Data for Advance Manufacturing Technology, Guizhou Normal College, Guiyang, 550018, China
- c) School of Chemistry and Chemical Engineering, Shandong University, Jinan 250100 China

**ABSTRACT:** Using density functional theory (DFT) calculations, we investigated O<sub>2</sub> activation by Au<sub>7</sub>-cluster supported on the perfect and hydroxyl defective Mg(OH)<sub>2</sub>(0001) surface. It is revealed that, hydroxyl groups on the perfect Mg(OH)<sub>2</sub>(0001) surface can not only enhance the stability of Au<sub>7</sub>-cluster, but also help the adsorption of O<sub>2</sub> molecule through hydrogen-bond interactions with the 2nd-layered interfacial Au sites. Density of states (DOS) analysis shows that the d-band centers of the 2nd-layered interfacial Au atoms are very close to the Fermi level, which thereby reduces the Pauli repulsion and promotes the O<sub>2</sub> adsorption. These two responses make the 2nd-layered interfacial Au atoms favor O<sub>2</sub> activation. Interestingly, the surface hydrogen atoms activated by the 1st-layered Au atoms can facilitate the O2 dissociation process as well. Such process is dynamically favorable and more inclined to occur in low temperatures than the direct dissociation process. Meanwhile, hydroxyl defects of Mg(OH)<sub>2</sub>(0001) locating right under the Au<sub>7</sub>-cluster can also shift up the d-band centers of the surrounding Au atoms toward the Fermi level, enhancing its catalytic activity for O<sub>2</sub> dissociation. On the contrary, the d-band

<sup>\*</sup> To whom all correspondences should be addressed. Tel: 86-851-86276007, Fax: 86-851-86276007, E-mail: cyjia@gznc.edu.cn; fwl@sdu.edu.cn.

center of Au atoms surrounding the hydroxyl defect near the  $Au_7$ -cluster exhibits an effective down-shift to lower energies, and therefore holds low activity. These results unveiled the roles of surface hydroxyls and hydroxyl defects on  $Au/Mg(OH)_2$  catalyst in  $O_2$  activation and could provide theoretical guidance for chemists to efficiently synthesize Au/hydroxide catalyst.

# 1. INTRODUCTION

Gold-based catalysts have received considerable attentions in the past decades because of their extraordinary activities in a wide variety of important catalytic conversions. [1-7] Among them, the catalytic oxidation reactions that use O<sub>2</sub> as oxidant have attracted the highest interest and are most extensively studied. [8-14] In this field, the general consensus is that the binding and activation of O<sub>2</sub> is the key elementary step with respect to catalytic activity. [15-17] However, as the most inert transition metal, pure gold surface is quite inactive for O<sub>2</sub> adsorption and activation. In order to improve the catalytic activity, various promotion measures have been investigated, such as the size and morphology control of gold particle, [18-21] the import of water vapor in the reaction stream, [22,23] and the optimization of preparation method. [24,25] Moreover, it is reported recently that the type and morphology of support are also crucial to activity. [26-30] Therefore, besides the above measures, the choice of suitable support for gold nanoparticles has become a good promoting method as well.

In recent years, gold nanoparticles on different supports have been extensively studied.<sup>[28-34]</sup> Among these multifarious types of supports, the hydroxide support is perhaps the most special one, since it provides a unique hydroxyl surface environment

for gold nanoparticles. It is found that the low temperature CO oxidation activity of gold nanoparticles on the hydroxide supports is much higher than that on the traditional oxide supports.<sup>[31-34]</sup> Therefore, the synthesis of Au/hydroxide catalysts is growing into new popular fields of study. To date, different promoting mechanisms regarding O<sub>2</sub> activation on Au/hydroxide catalysts have been proposed. On Au/Mg(OH)<sub>2</sub>, Haruta et al. conduct X-ray adsorption spectroscopy studies to show that the subnanometer gold clusters on the surface have large contribution to the Mg(OH)<sub>2</sub>-supported gold's activity.<sup>[35]</sup> By comparing to those typical Au/oxide catalysts (such as Au/MgO<sup>[36]</sup>, Au/SiO<sub>2</sub><sup>[37]</sup> and Au/TiO<sub>2</sub><sup>[38]</sup>), experimental studies revealed that the hydroxylation of support surface can effectively enhance the stability of small gold nanoparticles and further promote their catalytic activities.

All of those exciting experimental breakthroughs thus invoke many theoretical works aiming to get a clear and detailed explanation for the internal promoting mechanisms of hydroxyl groups. Simulation results have revealed that the generation of Au-OH bonds can enhance the stability of the composite catalyst and lead to effective charge transferring between gold nanoparticles and support. [39,40] However, there are still many important issues remaining unclear, such as the roles of hydroxyl groups in promoting the activity of gold nanoparticles, the oxygen binding and activation mechanisms on Au/hydroxide catalysts, and the effects of hydroxyl defects. The resolving of these issues will have important implications for the oxidation processes on Au/hydroxide catalysts.

In the present work, the Au/Mg(OH)<sub>2</sub> system is chosen as a model system to

perform density functional theory (DFT) calculations, so as to probe the catalytic roles of surface hydroxyl groups and hydroxyl defects in O<sub>2</sub> activation. Here the Mg(OH)<sub>2</sub> support offers an ideal hydroxyl platform to investigate the interactions between gold nanoparticles and hydroxyl groups. The majority of this work is aimed at gaining a detailed theoretical understanding of O<sub>2</sub> activation on the Au/hydroxide catalyst and of the main influence factors on its catalytic activities.

# 2. COMPUTATIONAL DETAILS AND MODELS

All the DFT calculations were performed by using codes from Vienna Ab Initio Simulation Package (VASP). The interactions between ions and electrons were described by the projector augmented wave (PAW) method. The Perdew-Burke-Ernzerhof (PBE) to functional was employed for the calculation of nonlocal exchange-correlation energy. A plane wave basis set with a cutoff energy of 400 eV was used for treating valence electrons, and the convergence criterion of energy was  $10^{-5}$  eV. Fully structural relaxation was performed until the forces on all unconstrained atoms were  $\leq 0.02$  eV/Å.  $2 \times 2 \times 1$  and  $9 \times 9 \times 1$   $\kappa$ -point grids determined by the Monkhorst–Pack were used for geometry optimization and DOS calculation, respectively. The transition states for the disassociation of  $O_2$  were searched by climbing image nudged elastic band (CI-NEB) method integrated in VASP. [46,47]

The optimized bulk  $Mg(OH)_2$  primitive cell parameters of a=b=3.142 Å, c=4.766 Å, were within 1% of the experimental values<sup>[48]</sup>, a=b=3.145 Å, c=4.769 Å. The (0001) surface of  $Mg(OH)_2$  was modeled using a 5 × 5 supercell with dimensions of 15.71 Å

 $\times$  15.71 Å  $\times$  19.10 Å. The perpendicular direction of the slab was separated by a 15 Å vacuum layer which was long enough to screen the self-interaction effects of the periodic boundary conditions. The two-dimensional (2D) Au<sub>7</sub>-cluster which was reported as a highly reactive cluster for CO oxidation <sup>[49]</sup> was optimized in a unit cell of 15 Å  $\times$  15 Å and only the  $\Gamma$ -point was used. The initial bond length and bond angle of Au<sub>7</sub>-cluster were referred to the Au(111) surface which was reported as a common exposed surface for Au clusters on Mg(OH)<sub>2</sub> support. <sup>[32,35]</sup> During geometry optimization, all the atoms in the slab were allowed to relax.

The binding energies of the adsorbates are calculated following the equation:

$$E_b = E_{sur+ad} - E_{sur} - E_{ad},$$

where

 $E_{\it sur+ad}$  is the total energy of the slab with the adsorbates on the surface,

 $E_{sur}$  is the total energy of the bare slab of the surface, and

 $E_{ad}$  is the total energy of the adsorbate species.

Therefore, a positive value of  $E_b$  means gaining energy during adsorption.

#### 3. RESULTS AND DISCUSSION

3.1. O<sub>2</sub> Adsorption and Dissociation on the Au<sub>7</sub>-Cluster Supported on Perfect Mg(OH)<sub>2</sub> (0001) Surface. The binding structures of Au<sub>7</sub>-cluster on Mg(OH)<sub>2</sub>(0001) surface are first examined. After trying a variety of possible composite configurations, four stable models were obtained, as seen in Figure 1. The optimized structures show that the generation of Au-OH bonds can significantly enhance the stability of the adsorption state and the binding energy increases with the number of Au-OH bonds,

which is consistent with previous studies<sup>[39]</sup>. Therefore, the **(Per-Au<sub>7</sub>-4)** state which contains more Au-OH bonds and has the lowest binding energy is chosen as the model system for further O<sub>2</sub> adsorption. From Figure 2, one can see that when the Au<sub>7</sub>-cluster is stably adsorbed on the Mg(OH)<sub>2</sub>(0001) surface, the d-band center of each Au atom is effectively shifted. It is known that the d-band states of the transition metal have great impacts on the interactions between the adsorbate and cluster.<sup>[28,50]</sup> The general rule is that the nearer of the d-band states of the transition metal is to the Fermi level, the stronger are the interactions with the adsorbate states. When the d-band states of the transition metal are up-shifted to the Fermi level, the antibonding states will be pushed above the Fermi level. This response can reduce the Pauli repulsion and make the bond between the adsobate and transition metal become more stable.<sup>[51]</sup> Therefore, the Au<sub>3</sub> and Au<sub>6</sub> atoms whose d-band states are much nearer to the Fermi level will be more favorable for O<sub>2</sub> adsorption than those un-shifted ones.

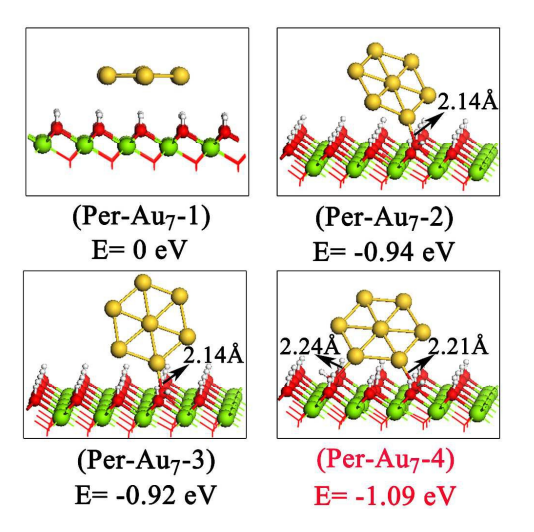


Figure 1. The four stable composite configurations and their relative binding energies of Au<sub>7</sub>-cluster on Mg(OH)<sub>2</sub>(0001) surface. Color coding: yellow, Au atoms; green, Mg atoms; red, O atoms; white, H atoms.

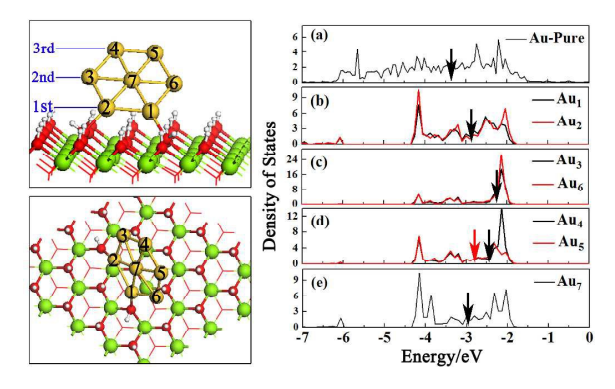


Figure 2. The side and top views of the most stable composite configuration of  $Au_7$ -cluster on  $Mg(OH)_2(0001)$  surface. Projected d-band states of each Au atoms are shown at the right side. The d-band center is marked by black or red arrow. The Fermi level is specified to 0 eV for all Au atoms. See Figure 1 for color coding.

After testing all the possible adsorption sites, the most stable adsorption states of O<sub>2</sub> on the cluster and at the interface between the cluster and the Mg(OH)<sub>2</sub>(0001) surface are obtained, as depicted in Figure 3 (the less stable states are shown in Figure S1). The binding structure in Figure 3-(Per-O<sub>2</sub>-1) shows that, on the Au<sub>7</sub>-cluster, the main force for anchoring O<sub>2</sub> is provided by the generation of Au-O bonds. However, at the interface (Figure 3-(Per-O<sub>2</sub>-2)), the bonds lengths of H-O<sub>II</sub> are 2.00 Å and 2.29 Å. They are close enough to each other to generate hydrogen bonds (about 1.5 Å-2.5 Å) which enhance the stability of the adsorption state. Therefore, at the interface, besides the generation of Au-O bonds, the generation of hydrogen bonds can promote the adsorption of O<sub>2</sub> as well. This just explains the fact that although the d-band center of Au<sub>4</sub> atom is nearly at the same position as Au<sub>6</sub> atom, the binding energy of (Per-O<sub>2</sub>-1) is 0.15 eV higher than (Per-O<sub>2</sub>-2). In addition, the O-O bond length in (Per-O<sub>2</sub>-1) and (Per-O<sub>2</sub>-2) has both been stretched (from 1.23 Å to 1.34 Å and 1.33 Å, respectively).

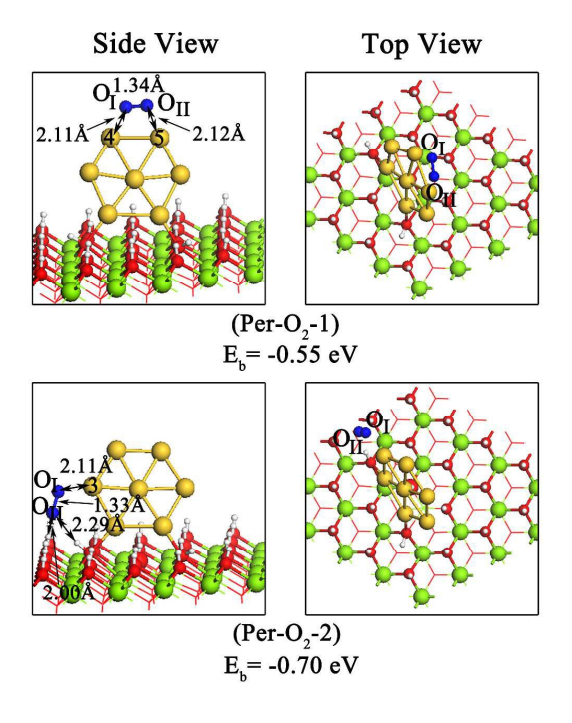


Figure 3. The side and top views of the most stable adsorption states of  $O_2$  on the Au<sub>7</sub>-cluster (**Per-O<sub>2</sub>-1**) and at the interfaces between the cluster and the Mg(OH)<sub>2</sub>(0001) surface (**Per-O<sub>2</sub>-2**). Color coding: blue, O atoms in adsorbed  $O_2$ ; others are the same as in Figure 1.

Having discussed the favorable molecular adsorption, we now turn to explore the dissociative process of  $O_2$ . The potential energy profile in Figure 4 shows that the dissociation of  $O_2$  on the  $Au_7$ -cluster is an exothermic process, by 0.22 eV, with an energy barrier of 2.15 eV. At the interface, the direct dissociation process of  $O_2$  is similar to the process in Figure 4, as shown in Figure 5-black line. However, its energy barrier (1.85 eV) is 0.30 eV lower than the former. This is because when  $O_2$  dissociated at the interface, the  $O_{II}$  atom can hardly move and hydrogen bonds exist all through the dissociation process. These enhance the stability of the transition state and lower the energy barrier. In addition, because the dissociated state (Per- $O_2$ -2-dis)

is more stable than (Per-O<sub>2</sub>-1-dis) (0.08 eV lower), the dissociation of O<sub>2</sub> at the interface will be more favorable both dynamically and thermodynamically. From Figure 5-red line, one can see that the surface H atoms which are activated by the 1st-layered Au atoms can participate in the reaction process as well (denoted as H-trans dissociation process). Our calculations show this only works for the H atoms in the Au-OH systems. For the other H atoms, no matter how we adjusted their positions, they easily go back to the surface O atoms after relaxation. For the activated H atom transferring on O<sub>2</sub>, it needs to overcome an energy barrier of 1.67 eV which is lower than the reaction process on the Au<sub>7</sub>-cluster and the direct dissociation process at the interface. Such process is endothermic, by 0.40 eV. The intermediate (H-trans) in Figure 5 shows that the O-O bond length has been stretched from 1.33 Å to 1.43 Å. This means that the pre-activation intensity of O<sub>2</sub> in this state has become larger than the molecular adsorption state at the interface (Per-O<sub>2</sub>-2). This response makes the further dissociation of O<sub>2</sub> become much easier. The energy barrier is only 1.55 eV, which is even lower than the H atom transfer process. This means that the rate-determining step of the H-trans dissociation process is the transfer of H atoms (TS 3). However, we need to point out that the final state (H-trans-dis) is less stable than state (Per-O<sub>2</sub>-2-dis), by 0.09 eV. Therefore, it is not difficult to come to a conclusion that the direct dissociation process is more favorable thermodynamically, while the H-trans dissociation process is more favorable dynamically. In other words, when temperature is low and time is short, the O<sub>2</sub> is more inclined to go through the H-trans dissociation process, however, as the temperature become higher and time

become longer, the direct dissociation process will get the upper hand.

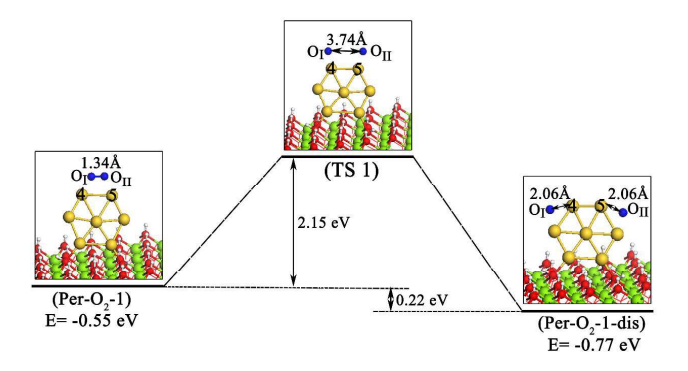


Figure 4. Potential energy profile for the dissociation of  $O_2$  on the  $Au_7$ -cluster supported on the perfect  $Mg(OH)_2(0001)$  surface. See Figure 3 for color coding.

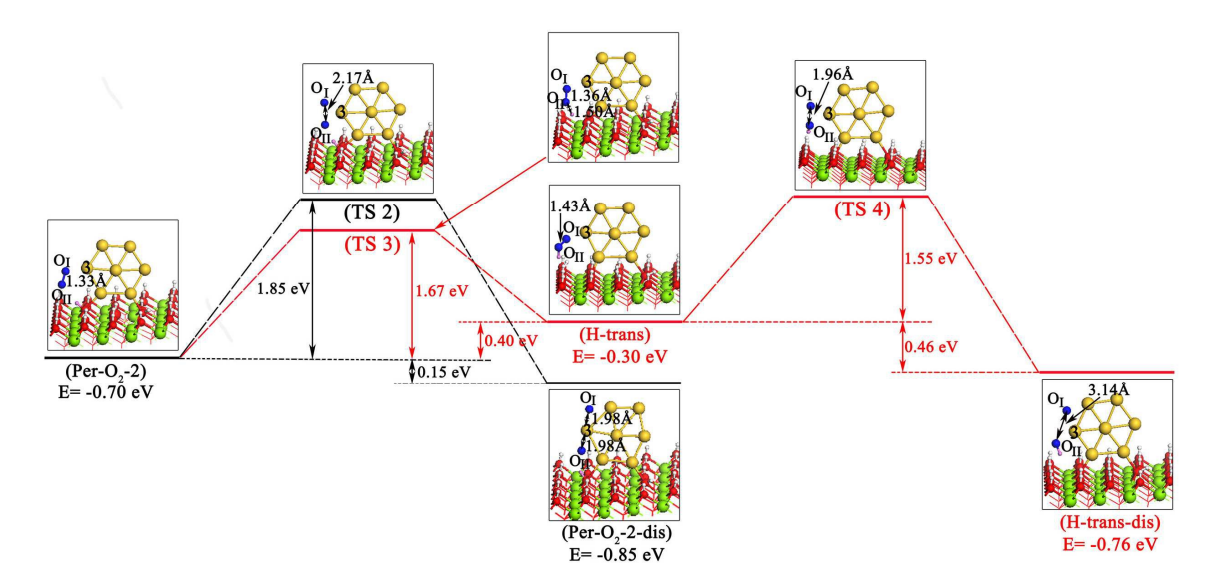


Figure 5. Potential energy profile for the dissociation of  $O_2$  at the interface between the  $Au_7$ -cluster and the perfect  $Mg(OH)_2(0001)$  surface. **Black line**: the direct dissociation process; **red line**: the H-trans dissociation process. Color coding: pink, the transferring H atom; others are the same as in Figure 3.

3.2. O<sub>2</sub> Adsorption and Dissociation on the Au<sub>7</sub>-Cluster Supported on Hydroxyl Defective Mg(OH)<sub>2</sub>(0001) Surface. Hydroxyl defect is an intrinsic defect in metal hydroxides, and it usually plays important roles in the catalytic activity of composite catalysts. On Mg(OH)<sub>2</sub>(0001) surface, two typical hydroxyl defects (the defect under (V<sub>OH</sub>-1) and near (V<sub>OH</sub>-2) the Au<sub>7</sub>-cluster) are investigated, as shown in Figure 6. After relaxation, the initial atomic and electronic structures of the Au<sub>7</sub>-cluster have changed. From Figure 7-(V<sub>OH</sub>-1-Au<sub>7</sub>), one can see that when Au<sub>7</sub>-cluster adsorbs on the Mg(OH)<sub>2</sub>(0001) surface with (V<sub>OH</sub>-1) defect, the Au<sub>2</sub> atom will be stretched out of the cluster and covers the defect site. This change makes the d-band center of Au<sub>2</sub> atom move much nearer to the Fermi level. Different from the (V<sub>OH</sub>-1-Au<sub>7</sub>) state, the structure of the (V<sub>OH</sub>-2-Au<sub>7</sub>) state has little distortion and the d-band center of the Au<sub>2</sub> atom which is near the hydroxyl defect has an effective down-shift to lower energies. Since the position of d-band center plays important roles in the catalytic activity, the differences between these two Au atoms lead to different activities for O<sub>2</sub>.

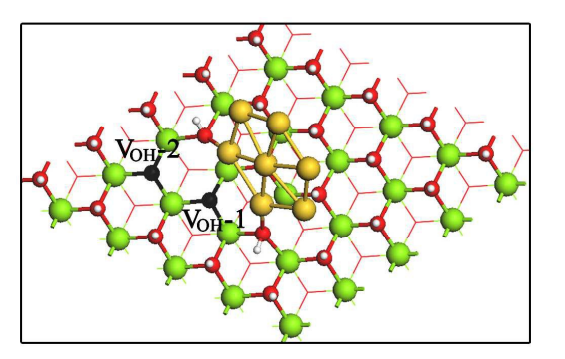


Figure 6. Two typical hydroxyl defects on Au/Mg(OH)<sub>2</sub> catalyst. Color coding: black, the hydroxyl defects; others are the same as in Figure 1.

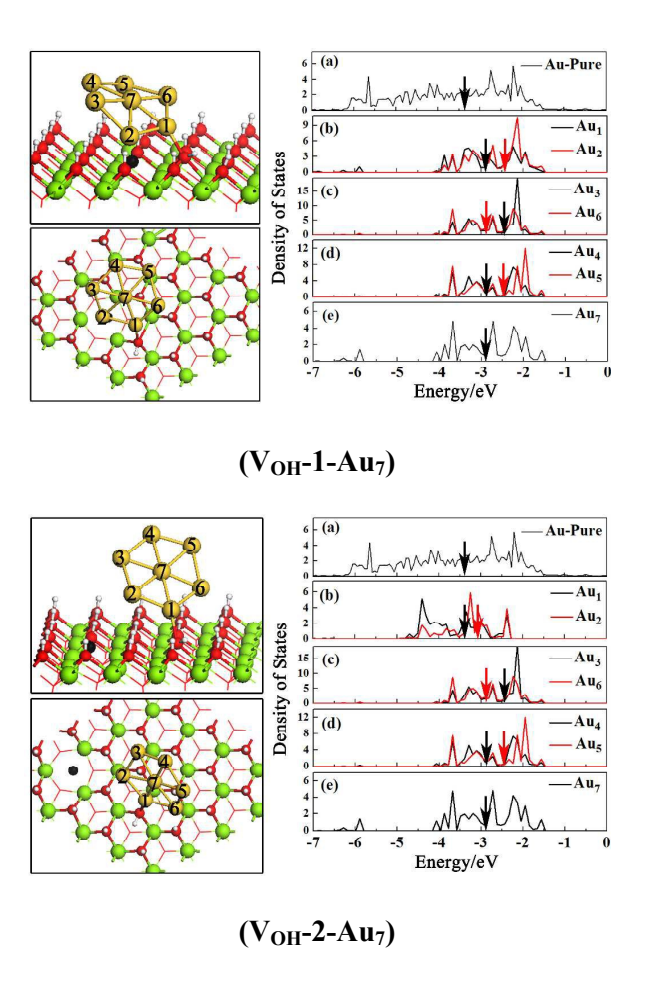


Figure 7. The side and top views of the optimized configuration of Au<sub>7</sub>-cluster on hydroxyl defective Mg(OH)<sub>2</sub>(0001) surface. Projected d-band states of each Au atoms are shown at the right side. The d-band center is marked by black or red arrow. The Fermi level is specified to 0 eV for all Au atoms. See Figure 6 for color coding.

After testing various binding forms of  $O_2$  on these two kinds of  $Au_2$  atom, the most stable one on each site is obtained, as depicted in Figure 8. The  $O_2$  adsorption state  $(V_{OH}-1-Au_7-O_2)$  is much more stable than state  $(V_{OH}-2-Au_7-O_2)$  and  $(Per-O_2-2)$  (Figure 3). This can be explained by two main reasons: one is that the  $O_2$  molecule is absorbed by two active Au atoms  $(Au_2$  and  $Au_3)$  in state  $(V_{OH}-1-Au_7-O_2)$  whose d-band centers are both close to Fermi level; the other is that the hydrogen bond in

state ( $V_{OH}$ -1- $Au_7$ - $O_2$ ) is much shorter and stronger than the hydrogen bonds in other states. The large binding forces between  $Au_2$  and  $Au_3$  atoms in  $Au_7$ -cluster and surface H atom have stretched the O-O bond length from 1.23 Å to 1.44 Å which is even longer than that in the intermediate (**H-trans**). Thus, when  $O_2$  adsorbs on this site, it will be significantly pre-activated as well. As for the other Au atoms, because their d-band centers are not effective changed, the adsorption behaviors of  $O_2$  on these sites are similar to the corresponding Au atoms in  $Au_7$ -cluster on the perfect  $Mg(OH)_2(0001)$  surface (as seen in Figure S2).

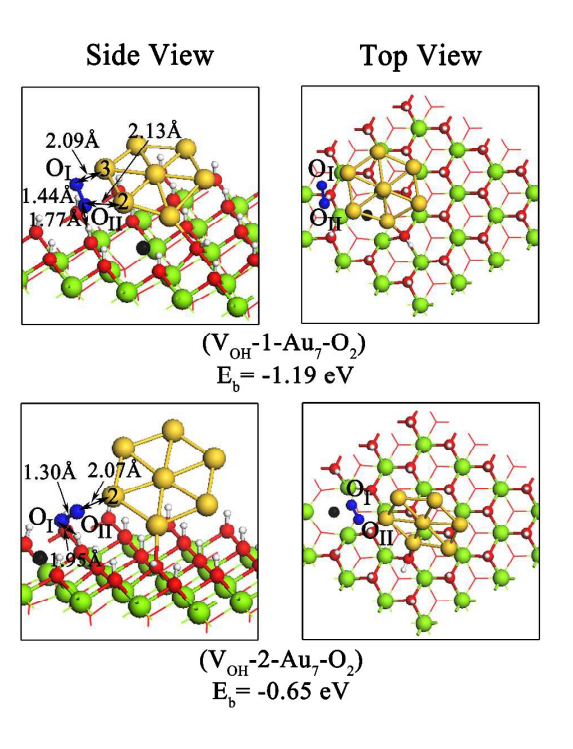


Figure 8. The side and top views of the most stable adsorption states of  $O_2$  on Au<sub>7</sub>-cluster supported on two kinds of hydroxyl defective Mg(OH)<sub>2</sub>(0001) surface. See Figure 3 and Figure 6 for color coding.

We have then investigated the dissociative process of O<sub>2</sub> on the defective surfaces.

The potential energy profiles and the corresponding transition states are shown Figure 9. It can be seen that the energy barrier of  $O_2$  dissociation on the ( $V_{OH}$ -1) defective surface is only 1.24 eV which is much lower than the rate-determining step of H-trans dissociation process (TS 3). This is because in TS 5 the hydrogen bond and the large binding forces of Au<sub>2</sub> and Au<sub>3</sub> atoms both have significant promotion for the stability of  $O_I$  and  $O_{II}$  atoms in  $O_2$ . Moreover, this process is exothermic, by 0.15 eV, and the stability of the final dissociated state (V<sub>OH</sub>-1-Au<sub>7</sub>-O<sub>2</sub>-dis) is much higher than that on the perfect surface as well (the binding energy is 0.49 eV lower than (Per-O<sub>2</sub>-2-dis) state in Figure 5). Therefore, the generation of (V<sub>OH</sub>-1) defect will make the dissociation of O<sub>2</sub> more dynamically and thermodynamically favorable than the perfect surface. For the dissociation process on the  $(V_{OH}-2)$  defective surface, the  $V_{OH}$ site will become a good site for anchoring  $O_2$ . However, the dissociation of  $O_2$  needs to overcome an energy barrier of 2.23 eV which is similar to **TS 1** in Figure 4 and this process is endothermic, by 0.38 eV. Thus, the catalytic activity of the Au atom near the  $(V_{OH}-2)$  defect is barely promoted.

From the above discussions, one can see that the hydroxyl defects under the  $Au_7$ -cluster can significantly enhance the catalytic activity surrounding Au atoms, while the defects near the cluster have little effect. Therefore, the hydroxyl defects generated on the synthesized  $Au/Mg(OH)_2$  catalyst can barely promote the catalytic activities of Au nanoparticles. Therefore, one should keep more hydroxyl defects on the support before Au clusters were deposited, so as to synthesize the most effective  $Au/Mg(OH)_2$  catalysts for  $O_2$  activation.

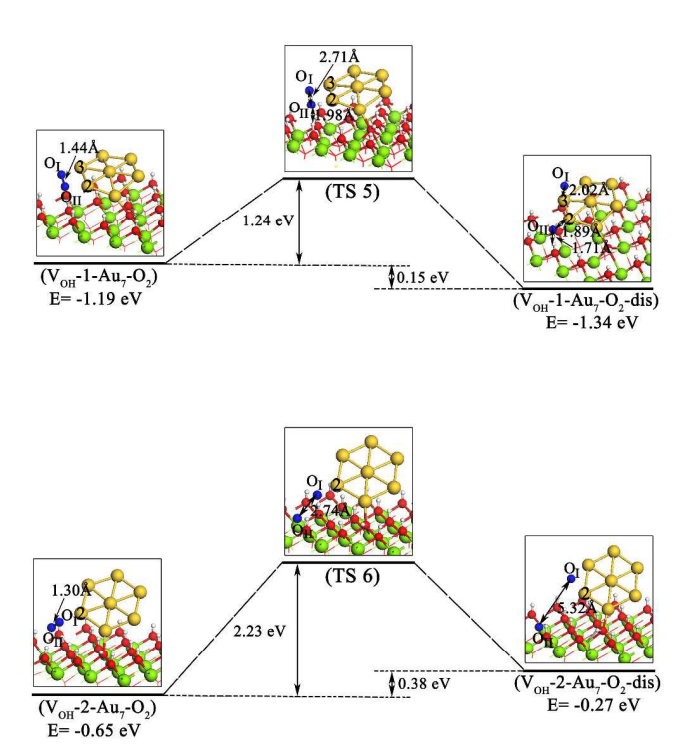


Figure 9. Potential energy profiles for the dissociation of  $O_2$  on the  $Au_7$ -cluster supported on the two typical hydroxyl defective  $Mg(OH)_2(0001)$  surfaces. Up:  $(V_{OH}-1)$ ; down:  $(V_{OH}-1)$ . See Figure 3 for color coding.

# 4. CONCLUSIONS

This work represents our theoretical attempt to rationalize the  $O_2$  activation process on  $Au/Mg(OH)_2$  catalyst, focusing on how surface hydroxyls and hydroxyl defects affect the reaction microscopically. The results show that the d-band states of the Au atoms play important roles in  $O_2$  adsorption and activation. Because the 2nd-layered interfacial Au atoms hold d-band centers are close to the Fermi level, the antibonding states of these Au atoms will be pushed above the Fermi level. Such response decreases the Pauli repulsion and enhances the stability and activity of the adsorbed

O<sub>2</sub>. Therefore, the 2nd-layered interfacial Au atoms are more active for O<sub>2</sub> activation.

The hydroxyl groups on Mg(OH)<sub>2</sub>(0001) surface can both enhance the stability of Au<sub>7</sub>-cluster and promote the adsorption and pre-activation of O<sub>2</sub> on the interfacial Au atoms. Furthermore, the hydrogen atoms activated by the Au atoms can directly participate in O<sub>2</sub> dissociation process as well. The energy barrier of this process is 0.18 eV lower than that of the direct dissociation process. Thus, the H-trans dissociation process will be more favorable dynamically. The hydroxyl defect right under the Au<sub>7</sub>-cluster can lead to significant up-shifts of the d-band center of the surrounding Au atoms, making them more favorable for O<sub>2</sub> activation. The hydroxyl defect near the Au<sub>7</sub>-cluster, however, offers little promotion effect for the surrounding Au atom.

In summary, our results demonstrate that the surface hydroxyl groups and hydroxyl defects on the Au/hydroxide catalysts are very influential for  $O_2$  adsorption and activation. To synthesize the most efficient Au/hydroxide catalysts for  $O_2$  activation, one should prepare more interfacial Au atoms (making the Au clusters have thin and flat structures) and generate more hydroxyl defects on supports before Au clusters were deposited.

**Supporting Information Available:** The less stable adsorption states of  $O_2$  on the  $Au_7$ -cluster and at the interface between the cluster and the perfect  $Mg(OH)_2(0001)$  surface, and the less stable adsorption states of  $O_2$  on the  $Au_7$ -cluster supported on the  $(V_{OH}-1)$  and  $(V_{OH}-2)$  defective  $Mg(OH)_2(0001)$  surface. This material is available free of charge via the Internet at <a href="http://pubs.acs.org">http://pubs.acs.org</a>.

#### Acknowledgment

This work is supported by the Natural Science Foundation of Guizhou Province (no. QKJ[2015]2129), the Construction Project for Guizhou Provincial Key Laboratories (Z[2013]4009), the GZNC startup package (no. 14BS022). We thank Prof. J. Jiang and W. H. Zhong for helpful discussions.

#### References

- (1) M. Haruta, Gold Bull., 2004, 37, 27-36.
- (2) J. T. Zhang, Y. Tang, K. Lee and M. Ouyang, *Science*, 2010, **327**, 1634-1638.
- (3) J. Sirijaraensre and J. Limtrakul, *Phys. Chem. Chem. Phys.*, 2015, 17, 9706-9715.
- (4) J. S. Lee, E. V. Shevchenko and D. V. Talapin, J. Am. Chem. Soc., 2008, 130, 9673-9675.
- (5) S. Carrettin, P. Concepcion, A. Corma, J. M. L. Nieto and V. F. Puntes, *Angew. Chem. Int. Ed.*, 2004, 43, 2538-2540.
- (6) N. Lopez and J. K. Nørskov, J. Am. Chem. Soc., 2002, 124, 11262-11263.
- (7) F. Vindigni, M. Manzoli, T. Tabakova, V. Idakiev, F. Boccuzzi and A. Chiorino, Phys. Chem. Chem. Phys., 2013, 15, 13400-13408.
- (8) A. Corma and H. Garcia, Chem. Soc. Rev., 2008, 37, 2096-2126.
- (9) A. S. K. Hashmi and G. J. Hutchings, Angew. Chem. Int. Ed., 2006, 45, 7896-7936.
- (10) M. Maciejewski, P. Fabrizioli, J. D. Grunwaldt, O. S. Becker and A. Baiker, *Phys. Chem. Chem. Phys.*, 2001, **3**, 3846-3855.
- (11) A. A. Herzing, C. J. Kiely, A. F. Carley, P. Landon and G. J. Hutchings, Science,

- 2008, **321**, 1331-1335.
- (12) J. L. C. Fajín, M. Natàlia, D. S. Cordeiro and J. R. B. Gomes, J. Phys. Chem. C, 2007, 111, 17311-17321.
- (13)B. Yoon, H. Häkkinen, U. Landman, A. S. Wörz, J. M. Antonietti, S. Abbet, K. Judai and U. Heiz, *Science*, 2005, **307**, 403-407.
- (14) M. Turner, V. B. Golovko, O. P. H. Vaughan, P. Abdulkin, A. Berenguer-Murcia,M. S. Tikhov, B. F. G. Johnson, R. M. Lambert, *Nature*, 2008, 454, 981-983.
- (15) M. C. Kung, R. J. Davis and H. H. Kung, J. Phys. Chem. C, 2007, 111, 11767-11775.
- (16) D. Widmann and R. J. Behm, Angew. Chem. Int. Ed., 2011, 50, 10241-10245.
- (17) K. L. Howard and D. J. Willock, Faraday Discuss., 2011, **152**, 135-151.
- (18) M. Valden, X. Lai and D. W. Goodman, Science, 1998, 281, 1647-1650.
- (19) M. S. Chen and D. W. Goodman, *Science*, 2004, **306**, 252-255.
- (20) M. S. Chen, Y. Cai. Z. Yan and D. W. Goodman, *J. Am. Chem. Soc.*, 2006, **128**, 6341-6346.
- (21)O. Lopez-Acevedo, K. A. Kacprzak, J. Akola and H. Häkkinen, *Nature Chem.*, 2010, **2**, 329-334.
- (22) S. T. Daniells, M. Makkee and J. A. Moulijn, *Catal. Lett.*, 2005, **100**, 39-47.
- (23) C. K. Costello, J. H. Yang, H. Y. Law, Y. Wang, J. N. Lin, L. D. Marks, H. H. Kung, *Appl. Catal. A: Gen.*, 2003, **243**, 15-24.
- (24) H. H. Kung, M. C. Kung and C. K. Costello, J. Catal., 2003, 216, 425–432.
- (25) S. H. Overbury, L. Ortiz-Soto, H. G. Zhu, B. Lee, M. D. Amiridis and S. Dai,

- Catal. Lett., 2004, 95, 99–106.
- (26) T. V. W. Janssens, A. Carlsson, A. Puig-Molina and B. S. Clausen, *J. Catal.*, 2006, 240, 108-113.
- (27) Z. P. Liu, P. Hu and A. Alavi, J. Am. Chem. Soc., 2002, 124, 14770-14779.
- (28) Z. P.; Liu, C. M. Wang and K. N. Fan, *Angew. Chem. Int. Ed.*, 2006, **45**, 6865-6868.
- (29) E. Florez, T. Gomez, J. A. Rodriguez and F. Illas, *Phys. Chem. Chem. Phys.*, 2011, 13, 6865-6871.
- (30) M. Haruta, S. Tsubota, T. Kobayashi, H. Kageyama, M. J. Genet and B. Delmon, J. Catal., 1993, 144, 175-192.
- (31) K. Qian, W. H. Zhang, H. X. Sun, J. Fang, B. He, Y. S. Ma, Z. Q. Jiang, S. Q. Wei, J. L. Yang and W. X. Huang, J. Catal., 2011, 277, 95-103.
- (32) D. A. H. Cunningham, W. Vogel and Haruta, M. Catal. Lett., 1999, 63, 43–47.
- (33) T. Takei, I. Okuda, K. K. Bando, T. Akita and M. Haruta, *Chem. Phys. Lett.*, 2010, **493**, 207–211.
- (34) C. J. Jia, Y. Liu, H. Bongard and F. Schüth, *J. Am. Chem. Soc.*, 2010, **132**, 1520-1522.
- (35) D. A. H. Cunningham, W. Vogel, H. Kageyama, S. Tsubota and M. Haruta, *J. Catal.*, 1998, **177**, 1–10.
- (36) M. A. Brown, E. Carrasco, M. Sterrer and H. J. Freund, J. Am. Chem. Soc., 2010, 132, 4064–4065.
- (37) H. G. Zhu, Z. Ma, J. C. Clark, Z. W. Pan, S. H. Overbury and S. Dai, Appl., Catal.

- A: Gen. 2007, **326**, 89–99.
- (38) G. M. Veith, A. R. Lupini and N. J. Dudney, *J. Phys. Chem. C*, 2009, **113**, 269–280.
- (39) D. E. Jiang, S. H. Overbury and S. Dai, J. Phys. Chem. Lett., 2011, 2, 1211–1215.
- (40) W. Vogel, D. A. H. Cunningham, K. Tanaka and M. Haruta, *Catal. Lett.*, 1996, **40**, 175-181.
- (41) G. Kresse and J. Furthmüller, *Phys. Rev. B*, 1996, **54**, 11169–11186.
- (42) P. E. Blöchl, *Phys. Rev. B*, 1994, **50**, 17953–17979.
- (43) G. Kresse and D. Jouber, *Phys. Rev. B*, 1999, **59**, 1758–1775.
- (44)O. Bengone, M. Alouani, P. E. Blöchl, J. Hugel, Phys. Rev. B, 2000, 62, 16392–16401.
- (45) J. P. Perdew, K. Burke and M. Ernzerhof, *Phys. Rev. Lett.*, 1996, 77, 3865–3868.
- (46) G. Mills, H. Jonsson and G. K. Schenter, Surf. Sci., 1995, 324, 305-337.
- (47) G. Henkelman, B. P. Uberuaga and H. Jónsson, J. Chem. Phys., 2000, 113, 9901-9904.
- (48) T. S. Duffy, J. F. Shu, H. K. Mao and R. J. Hemley, *Phys. Chem. Miner.*, 1995, **22**, 277–281.
- (49) S. Lee, C. Fan, T. Wu and S. L. Anderson, *J. Am. Chem. Soc.*, 2004, **126**, 5682–5683.
- (50) Z. P. Liu, X. Q. Gong, J. Kohanoff, C. Sanchez and P. Hu, *Phys. Rev. Lett.*, 2003, 91, 266102-266105.
- (51) J. P. Xiao and T. Frauenheim, J. Phys. Chem. C, 2013, 117, 1804–1808.